

Lattice effects and current reversal in superconducting ratchets

This content has been downloaded from IOPscience. Please scroll down to see the full text.

2007 New J. Phys. 9 366

(<http://iopscience.iop.org/1367-2630/9/10/366>)

View [the table of contents for this issue](#), or go to the [journal homepage](#) for more

Download details:

IP Address: 147.96.14.15

This content was downloaded on 28/04/2015 at 18:09

Please note that [terms and conditions apply](#).

Lattice effects and current reversal in superconducting ratchets

L Dinis¹, E M González², J V Anguita³, J M R Parrondo¹
and J L Vicent²

¹ Grupo Interdisciplinar de Sistemas Complejos (GISC) and Departamento de Física Atómica, Nuclear y Molecular, Universidad Complutense de Madrid, E-28040 Madrid, Spain

² Departamento de Física de Materiales, Universidad Complutense de Madrid, E-28040 Madrid, Spain

³ Instituto de Microelectrónica de Madrid, Consejo Superior de Investigaciones Científicas, Tres Cantos, E-28760, Spain

E-mail: ldinis@fis.ucm.es

New Journal of Physics **9** (2007) 366

Received 27 June 2007

Published 9 October 2007

Online at <http://www.njp.org/>

doi:10.1088/1367-2630/9/10/366

Abstract. Competition between the vortex lattice and a lattice of asymmetric artificial defects is shown to play a crucial role in ratchet experiments in superconducting films. We present a novel and collective mechanism for current reversal based on a reconfiguration of the vortex lattice. In contrast to previous models of vortex current reversal, the mechanism is based on the global response of the vortex lattice to external forces.

Contents

1. Introduction	2
2. Experimental method	3
3. Theoretical model	4
4. Discussion: vortex lattice reconfiguration and current reversal	7
5. Conclusions	11
Acknowledgments	11
References	11

1. Introduction

The term *ratchet effect* refers to a net flow of particles induced by asymmetric potentials, in the absence of non-zero average forces. This effect has drawn the attention of many researchers from very different fields [1]. It is believed to play a role in protein motors [2] and it has been used to design synthetic molecular motors [3, 4] and control the motion of colloidal particles [5].

In the context of superconductivity, vortices in superconducting films [6, 7] and Josephson junctions [8, 9] were soon proposed as implementations of the ratchet effect. The first experimental evidence of rectification of vortices was reported by Villegas *et al* [10]. In this work, a Nb superconducting film was grown on an array of triangular Ni nanoislands, acting as pinning sites for the vortices. When the vortex lattice is driven by an input ac-current, the asymmetric geometry of the pinning potential leads to a net flow of vortices, resulting in an output dc-voltage. After this seminal work, considerable theoretical [11]–[13] and experimental [14] research has been done in order to clarify ratchet mechanisms or use them to control the motion of vortices in films and Josephson arrays.

An interesting feature of this experimental set-up is the appearance of current reversals, i.e. the rectification polarity changes for certain values of the applied magnetic field and current strength. This behavior has been explained in [10] by means of a one-dimensional (1D) model, where current reversal is due to the interplay between vortices pinned in the asymmetric centers (triangles) and interstitial vortices placed among the triangles. However, in that model the interaction between pinned and interstitial vortices was replaced by an effective ratchet potential affecting only interstitial vortices. Beside this effective potential, both pinned and interstitial vortices were treated as independent particles.

In the present paper, we review the experimental results of Villegas *et al* [10] of rectification and current reversal using magnetic defects, and present experimental results showing that the current reversal persists with non-magnetic defects. Furthermore, we introduce a new theoretical approach to the current reversal considering interaction between vortices. In the absence of pinning potentials, it is well known that the ground state induced by vortex interaction is a triangular Abrikosov lattice [15]. Our aim is to analyze how this vortex lattice is distorted by the lattice of asymmetric defects. The competition between the two lattices will be relevant when the magnetic field creates a few vortices per pinning site and for long penetration depth, λ , which is the case for temperatures close to the critical temperature, as in the experiments reported in [10]. Furthermore, we will show that this vortex lattice distortion can induce current reversal but nevertheless the lattice exhibits a net motion, i.e. both pinned and interstitial vortices move in the same direction. Therefore, our picture of vortex rectification and current reversal differs both from the one presented in [10], where the latter is induced only by the motion of interstitial vortices, and that in [11, 16] which deal with systems of particles where by adding particles of an auxiliary species, that interact with both the primary ones and the substrates, the particles could move either together or in opposite directions depending upon the strength of the interaction, and whether it is attractive or repulsive.

Moreover, in our new approach, the superconductor ratchet becomes a collective ratchet. Collective effects in ratchets have been shown to yield new interesting phenomena such as instabilities and hysteresis [2], absolute negative resistance [17] and inefficiency of some feedback control protocols [18]. Moreover, many biological motors, such as kinesins and myosins, work in a collective way [2]. Collective effects have been also considered in the context of superconducting vortices by Reichhardt *et al* [19] and de Souza Silva *et al* [20]. Also Shalom

and Pastoriza suggested that collective effects are responsible for current reversal in Josephson junction arrays [21].

In our approach, we show that current reversal corresponds to a reconfiguration of the vortex lattice at different fields and drives. Similar arguments about the importance of the vortex–vortex interactions in current reversal mechanisms were made in [19]. In their simulations they observe how interstitial vortices may help depin vortices at the tip of the triangular defect due to thermal fluctuations but not the ones at the base of the triangle, leading to a negative current at low drives. Also, the current reversal is explained by vortex–vortex interactions in the framework of a 1D model in [20]. However, none of these works discuss the aforementioned competition between the Abrikosov lattice and the array of defects.

Recently, Lu *et al* [22] have reported a vortex ratchet effect for a (2D) vortex system interacting with a substrate that has an asymmetric periodic modulation along one direction. Although the pinning in that system might be expected to have a 1D character, Lu *et al* showed that the ratchet effect and current reversals are produced by collective vortex–vortex interactions, and also showed that the overall vortex lattice structure can change for drives in the opposite direction.

The paper is organized as follows. In section 2, we review the experiment and present results with Cu non-magnetic artificial defects. In section 3, we introduce the model used in numerical simulations. In section 4, we discuss current reversal and lattice configurations. Finally, we present our conclusions in section 5.

2. Experimental method

We have fabricated the Nb thin films on top of arrays of Cu or Ni nanotriangles grown on Si (100) substrates, by means of electron beam lithography, magnetron sputtering and ion etching techniques [10, 23]. The array aspect ratio and the triangle dimensions of the samples are similar to the films reported by Villegas *et al* [10]: the periodicity of the array is $770\text{ nm} \times 746\text{ nm}$, the triangle base is 620 nm and height is 477 nm . A cross-shaped patterned bridge allows us to inject a current into the sample and measure the voltage drop parallel or perpendicular to the triangle base. In all the experiments, the magnetic field H is applied perpendicular to the substrate. In the ratchet measurements, an injected ac current is applied and the output dc voltage is recorded, whereas a commercial He cryostat is used to control the temperature. More fabrication and characterization details have been reported elsewhere [10, 23].

The dc magnetoresistance of superconducting thin films with periodic arrays of pinning centers shows minima when the vortex lattice matches the unit cell of the array [24]. These minima are sharp (strong reduction of the dissipation) and equally spaced (two neighbor minima are always separated by the same magnetic field value). Consequently, the number of vortices per array unit cell can be known by simple inspection of the dc magnetoresistance $R(H)$ curves, in which the first minimum corresponds to one vortex per unit cell, the second minimum to two vortices per unit cell, and so on. Moreover, the ratio between the dimension of the pinning center and the superconducting coherence length governs the maximum number of vortices that could be pinned in each one of the pinning centers [25]. The dimensions of our defects allow a maximum of three pinned vortices per triangle. Therefore, increasing the applied magnetic field to four vortices per array unit cell leads to three pinned vortices and one interstitial vortex [10]. In general, we know, for selected values of the applied magnetic field, how many vortices

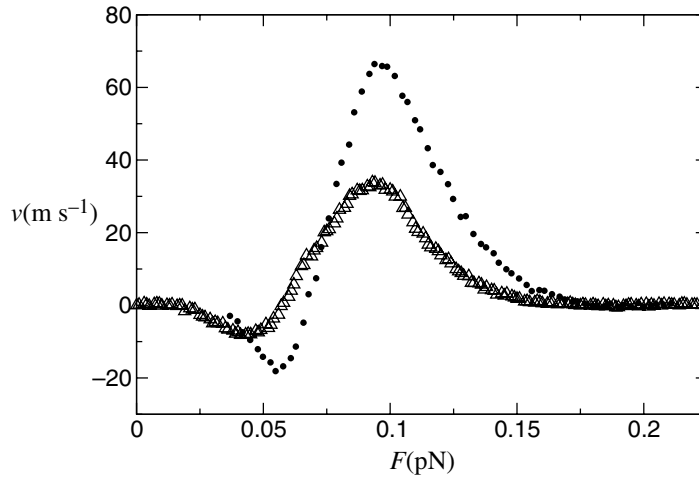


Figure 1. Velocity vs driving force for an applied magnetic field is $H = 1.3 \times 10^{-2}$ T ($n = 4$ vortices per array unit cell) and temperature $T/T_c = 0.99$. The ac current frequency is 10 kHz. The sample is a Nb film 100 nm thick with array of 40 nm thick triangles (array periodicity $770 \text{ nm} \times 746 \text{ nm}$, triangle side 620 nm). Dots: Nb film with array of Ni triangles. Triangles: Nb film with array of Cu triangles.

there are per unit cell and how many of them are pinned and interstitial in the ground state and for zero external force. We have to notice that, in this type of experiment, the periodic potentials govern the vortex dynamics inducing many remarkable effects, such as vortex lattice reconfiguration [26] or vortex lattice channeling effects [27]. Finally, we have used different frequencies, up to 10 kHz, for the input signal with identical results. This indicates that our experiments are carried out in the adiabatic regime [14, 23], i.e. the period of the signal is much longer than the relaxation time of the system, which is able to adopt the corresponding stationary state at any time.

Figure 1 shows the experimental results of Nb films on arrays of Ni (magnetic) and Cu (non-magnetic) nanotriangles for $n = 4$ vortices per triangle. The results corresponding to Ni defects are similar to those reported in [10] with a clear current reversal. The Cu non-magnetic defects exhibit a similar behavior. In this type of defect, pinning is weaker [28] and, consequently, rectification is lower and depinning forces are smaller.

3. Theoretical model

To clarify the mechanisms behind the experimental results, we have performed extensive numerical simulations of vortices as a set of interacting and overdamped 2D Brownian particles. Similar simulations have been used to study the dc vortex transport properties of arrays of triangular pinning antidots [29] and current reversal in arrays of triangular pinning defects [19], although in these references the effects of possible lattice reconfigurations are not analyzed.

The corresponding Langevin equation for position r_i of vortex i reads:

$$\eta \dot{\mathbf{r}}_i(t) = - \sum_{j \neq i} \vec{\nabla}_i U_{vv}(|\mathbf{r}_i - \mathbf{r}_j|) + \mathbf{F}_{\text{pinn}}(\mathbf{r}_i) + \mathbf{F}_{\text{ext}}(t) + \mathbf{\Gamma}_i(t), \quad (1)$$

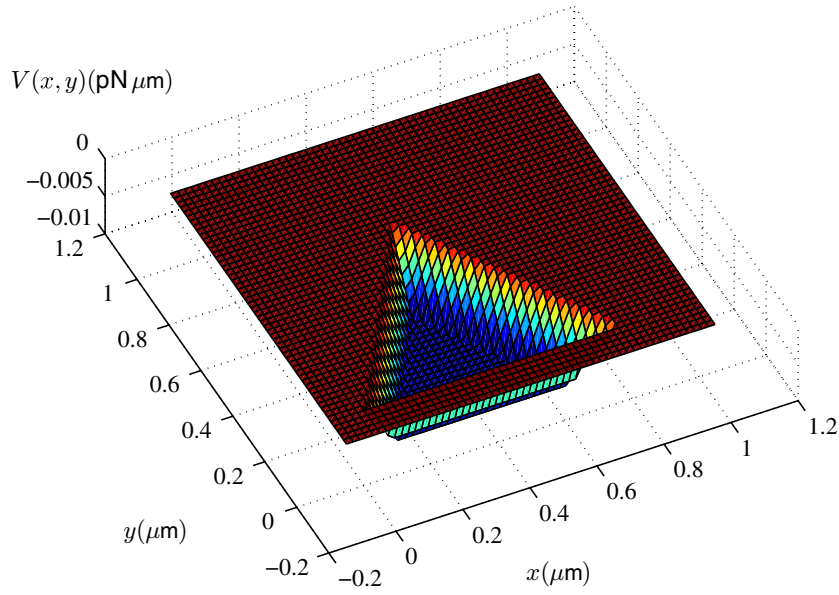


Figure 2. Potential acting on vortices due to pinning defects.

where η is the viscosity, $U_{\text{vv}}(r)$ is the interaction potential between vortices, $\mathbf{F}_{\text{pinn}}(\mathbf{r})$ the force due to pinning artificial defects, $\mathbf{F}_{\text{ext}}(t)$ the external force due to the applied currents, and $\Gamma_i(t)$ is white Gaussian noise accounting for thermal fluctuations:

$$\langle \Gamma_i(t) \cdot \Gamma_j(t') \rangle = 4kT\eta\delta_{ij}\delta(t-t'). \quad (2)$$

For the vortex interaction potential, we have used [16]:

$$U_{\text{vv}}(r) = \frac{\phi_0^2}{4\pi\mu_0\lambda^2} K_0\left(\frac{r}{\lambda}\right), \quad (3)$$

where $\phi_0 = hc/(2e)$ is the quantum of flux, μ_0 is the magnetic permeability of vacuum, K_0 is the zeroth-order modified Bessel function, and λ is the penetration depth of the material, which is very sensitive to temperature for the conditions of the experiment, very close to the critical temperature.

The external force \mathbf{F}_{ext} is the Lorentz force resulting from the applied current. As in the experiment, this force is perpendicular to the basis of the triangles and sinusoidal in time.

The triangular pinning defects have been simulated using an attractive potential in the shape of an inverted triangular truncated pyramid, that is, null force in the middle section of the triangle, and constant force F_p pointing inward in a region of width d along the walls of the pinning defect (see figure 2). We have used an array of 6×6 defects with periodic boundary conditions.

The parameters in the simulation have been chosen similar to already reported values in samples of Nb films with arrays of periodic pinning centers [30]. We take $\lambda = 360 \text{ nm}$ and temperature $T = 8.26 \text{ K}$, which are typical values close to the superconducting critical temperature. The pinning strength $F_p = 0.12 \text{ pN}$ and the width of the pinning potential $d = 0.7 \mu\text{m}$ have been set so that vortices start depinning approximately at the same applied force as observed in the experiment (see [10]), whereas the dimensions of the triangles in the simulation correspond to those in the experiment. We point out that nevertheless simulations performed with small variations on these parameters exhibit similar behavior.

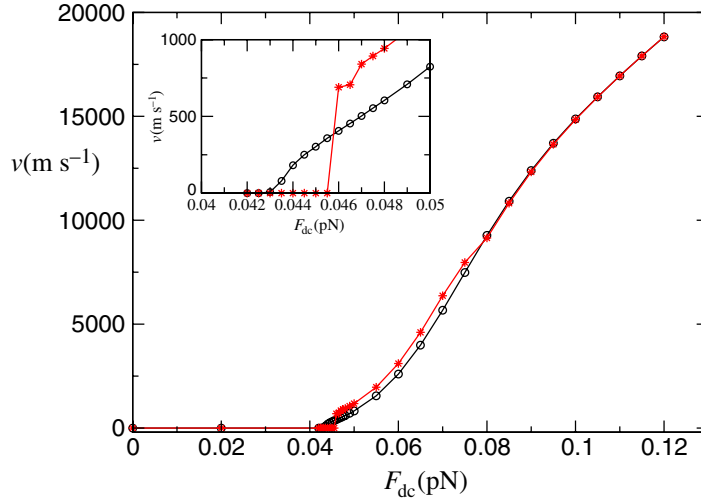


Figure 3. Velocity (absolute value) of the lattice as a function of the applied force, for positive (*) and negative (o) forces. Simulation results and linear interpolation. Inset shows the inversion in more detail.

Finally, we have followed the suggestion made in [31] introducing a viscosity $\eta(F)$ depending on the strength of the external force. The reason for this dependence is that viscosity is in fact the result of the interaction of vortices with random intrinsic pinning centers scattered all over the material. To mimic the behavior of the viscosity measured in [31], we have taken in our simulations the following phenomenological expression for the viscosity:

$$\eta(F) = (0.005 e^{-100|F(\text{pN})|} + 6 \times 10^{-6}) \text{ pN s m}^{-1}. \quad (4)$$

Notice however that the viscosity enters in the Langevin equation (1) as a time scale. Therefore, it affects the magnitude of the velocity of the vortices, but not the qualitative behavior of the lattice or the mechanisms that lead to current reversal.

As mentioned above, our experimental results, in agreement with previous work [14, 23], show that the system is adiabatic in the region of applied frequencies, which allowed us to perform our simulations also in the adiabatic limit. We first obtain $v_{\text{dc}}(F)$ curves for different values of constant positive and negative forces (dc curves). These dc curves are depicted in figure 3, where the absolute value of the velocity of the vortex lattice is plotted against the applied force. The inversion is clearly shown in the inset. Once the dc curves are obtained, the corresponding ac curves $v_{\text{ac}}(F_{\text{ac}})$ can be easily computed by performing the following numerical integration which does not depend on the frequency of the force (throughout the paper F_{ac} stands for the rms value of the external force):

$$v_{\text{ac}}(F_{\text{ac}}) = \int_0^{2\pi} v_{\text{dc}}(F_{\text{ac}}\sqrt{2}\sin(t))dt. \quad (5)$$

Figure 4 shows the average velocity for 144 particles and 6×6 pinning triangles ($n = 4$) and the parameters described above, as a function of the external force F_{ac} . Simulations reproduce the experimentally observed current reversal, i.e. negative current for smaller forces and positive current for higher forces, decaying to zero afterward. Furthermore, the forces applied and the corresponding velocities are both quite similar to those in the experiment.

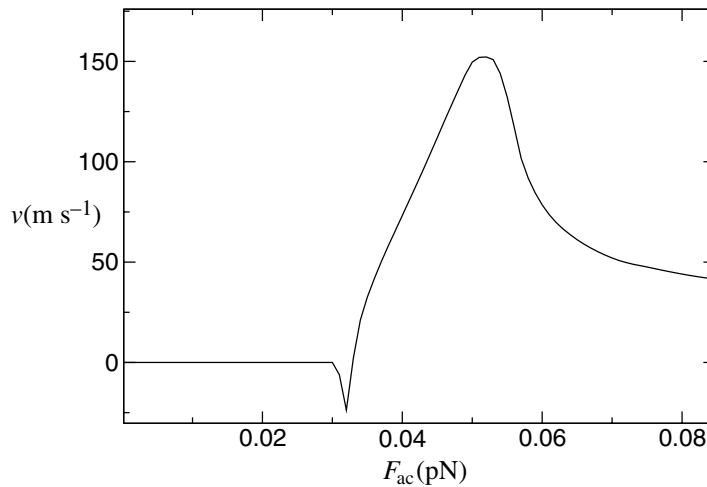


Figure 4. Average velocity of the vortices as a function of the rms amplitude F_{ac} of the external force.

4. Discussion: vortex lattice reconfiguration and current reversal

Consider a single particle or vortex in the triangular potential of figure 2. The force to depin the vortex when pushing in the positive y -direction through the tip of the triangle is approximately half the force needed to depin it through the base, when pushing in the negative y -direction. Positive or upward is therefore the ‘natural’ direction for the rectification induced by triangular defects, and it is observed experimentally for $n = 1, 2, 3$ [10]. However, as shown in figure 1, for $n = 4$ downward rectification is also observed for small forces, and the same unexpected result is obtained for $n \geq 4$ [10].

What is the mechanism of this negative rectification? Previous models [10] consider that the interstitial vortices feel an effective ratchet potential which is roughly the spatial inverse of the pinning potential, so they are rectified in the negative direction and move independently of the pinned vortices. However, a simple visual inspection of our simulations reveal that the lattice moves as a whole without significant shear and that current reversal is due to a reconfiguration of the vortex lattice (see [supplementary multimedia material](#)).

In figure 5(a), we depict the vortex lattice that minimizes the total free energy and has the periodicity of the rectangular array of triangles, for $n = 4$ and zero external force. We have found this configuration by simulated annealing on a cell with a single defect and periodic boundary conditions. Notice that the actual ground state or minimal energy configuration might not in principle have the periodicity of the array of defects, especially for weak pinning forces. However, our simulations reveal that this is not the case for the parameters chosen above: figure 5(a) is indeed the ground state of the system, consisting of a slightly distorted triangular lattice (vortices form isosceles triangles but no equilateral) with one interstitial and three pinned vortices.

This lattice starts to move either upward or downward if we add a force, but it turns out that the depinning force is stronger in the positive direction, yielding a negative rectification.

The effect can be explained by considering first a rigid lattice. When pushing upward (toward the positive y -direction) the y -component of the total force acting on the three pinned vortices due to the pinning is $-3F_p \cos \alpha$ (figure 5(b)), α being the angle at the basis of the

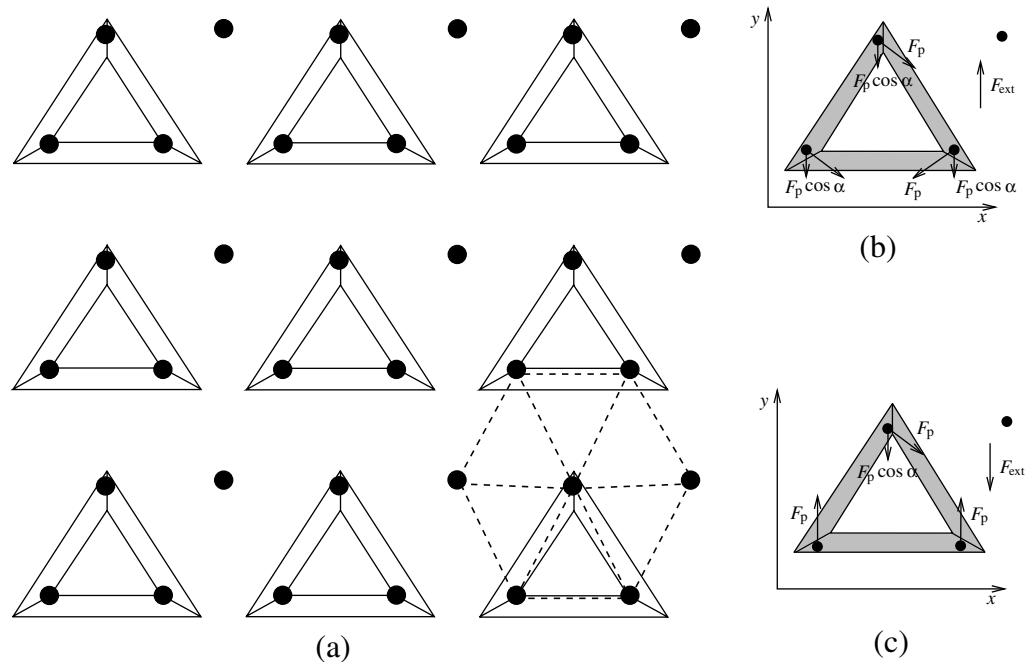


Figure 5. The ground state of the system for zero external force.

triangle. On the other hand, for a negative motion, the total force to overcome in the y -direction is $(2 - \cos \alpha)F_p$ (figure 5(c)). In the case of equilateral triangles, $\cos \alpha = 1/2$ and both depinning forces are identical. Our triangles are however a little bit flattened, with base 620 nm and height 477 nm. Using these values and $F_p = 0.12$ pN, the resulting depinning forces per vortex are 0.0437 pN (downward) and 0.0490 pN (upward).

Although this argument is only valid for zero temperature and a rigid lattice, the depinning forces observed in the simulation (figure 4) are very close to these estimated values: we observe downward depinning for 0.0435 pN and upward for 0.0460 pN. The greater discrepancy for the upward motion indicates that the plasticity of the lattice is more relevant in the upward depinning, whereas the lattice is barely deformed in the downward motion. In the [supplementary multimedia material](#), one can see how the whole lattice remains pinned for an external force $F = 0.044$ pN, whereas it does move downward for the same negative force $F = -0.044$ pN with a small deformation. We then conclude that the negative rectification is mainly due to the shape of the triangular defects.

Increasing the external force we get upward rectification. For $F = 0.05$ pN, the lattice is already depinned in the upward direction, but we observe a very interesting phenomenon which is the main result of the paper: the lattice undergoes a transition (see [supplementary multimedia material](#)) adopting the configuration depicted in figure 6 with only one (or two at most) pinned vortices. This new configuration is the result of a 90° rotation of the ground state of figure 5, and induces a relatively fast columnar motion of vortices which exceeds the motion in the downward direction for the same magnitude of the external force, yielding a net upward rectification.

Therefore, our simulations reveal that the current reversal is entirely due to a reconfiguration of the vortex lattice. Changes in lattice configuration have been extensively reported in the literature, mainly in equilibrium [26, 32, 33]. In our case, however, the

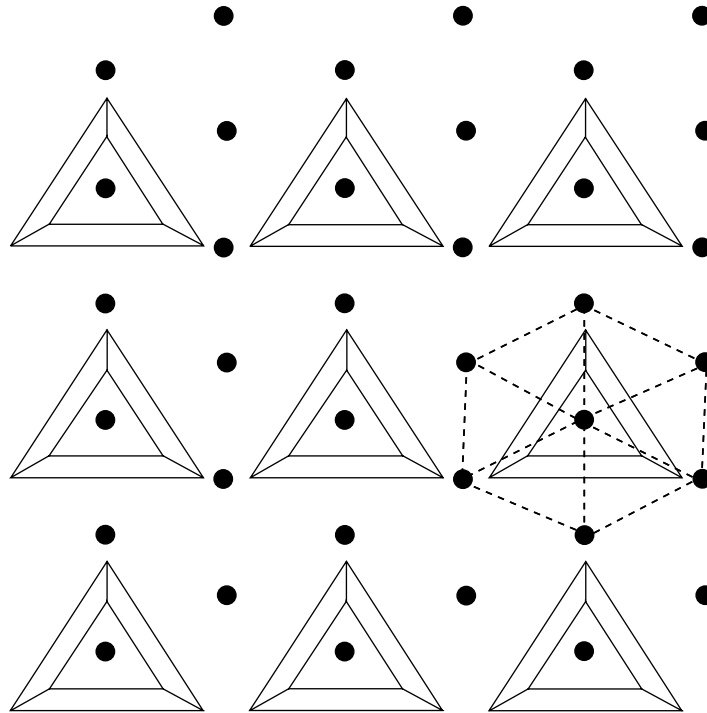


Figure 6. Configuration for $F_{\text{ext}} = 0.1$ pN.

reconfiguration is a dynamical phenomenon. In spite of this, we can gain some insight on the problem by calculating the interaction energy of the configurations depicted in figures 5 and 6 and comparing it with the interaction energy of triangular and square lattices with the same density of vortices.

Let a and b be respectively the horizontal and vertical distance between triangles in the array of defects. The lattice in figure 5 (we will call it lattice H) is given by $n\mathbf{v}_{\text{H},1} + m\mathbf{v}_{\text{H},2}$, with $n, m = 0, \pm 1, \pm 2, \dots$ and the following generating vectors:

$$\mathbf{v}_{\text{H},1} = \begin{pmatrix} a/2 \\ 0 \end{pmatrix}; \quad \mathbf{v}_{\text{H},2} = \begin{pmatrix} a/4 \\ b/2 \end{pmatrix}. \quad (6)$$

The corresponding generating vectors for the lattice in figure 6, denoted as V, are:

$$\mathbf{v}_{\text{V},1} = \begin{pmatrix} a \\ 0 \end{pmatrix}; \quad \mathbf{v}_{\text{V},2} = \begin{pmatrix} a/2 \\ b/4 \end{pmatrix}. \quad (7)$$

One can show that, for a square array of defects, i.e. $a = b$, lattice H is a 90° rotation of lattice V and the interaction energy is obviously identical.

The ground state of the system without triangular defects is a regular triangular lattice T with vortex density σ , whose generating vectors can be written as:

$$\mathbf{v}_{\text{T},1} = \begin{pmatrix} \sqrt{\frac{2}{\sigma\sqrt{3}}} \\ 0 \end{pmatrix}; \quad \mathbf{v}_{\text{T},2} = \begin{pmatrix} \sqrt{\frac{1}{2\sigma\sqrt{3}}} \\ \sqrt{\frac{\sqrt{3}}{2\sigma}} \end{pmatrix}. \quad (8)$$

For an aspect ratio $b/a = \sqrt{3}/2$, the vortex density is $\sigma = 8/(a^2\sqrt{3})$ and lattice H coincides with the regular triangular lattice T. For $b/a = 2/\sqrt{3}$, one can also prove that lattice V becomes

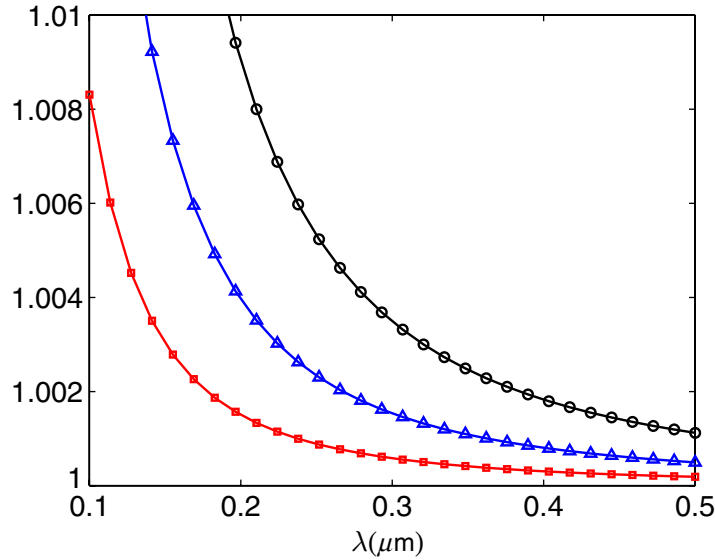


Figure 7. Interaction energy for the H, V and R lattices compared to the regular triangular one, T: E_H/E_T (red squares), E_V/E_T (blue triangles), E_R/E_T (black circles). Computed numerically to convergence, including 10 000 neighbors.

regular. Therefore, any deviation (as in our experiment) from these aspect ratios induces a distortion in the lattices in order to conform with the periodicity of the array. In fact, since the aspect ratio of the array in the experiment and simulations $b/a = 746/770 = 0.969$ is closer to $\sqrt{3}/2$ rather than to $2/\sqrt{3}$, H is less distorted than V.

Another trivial way of conforming to the periodicity of the array with $n = 4$ vortices per defect, is the rectangular lattice R generated by:

$$\mathbf{v}_{R,1} = \begin{pmatrix} a/2 \\ 0 \end{pmatrix}; \quad \mathbf{v}_{R,2} = \begin{pmatrix} 0 \\ b/2 \end{pmatrix}. \quad (9)$$

We have evaluated the interaction energy, E_H , E_V , E_T , E_R , of these four lattices for the values $a = 770$ nm, $b = 746$ nm and $\sigma = 4/(ab)$ corresponding both to the experiment and simulations. The energies are very close to each other. In figure 7 we plot the energies compared to the ground state T, i.e. the ratios E_H/E_T , E_V/E_T , E_R/E_T , as a function of λ . As expected, the minimal interaction energy corresponds to the regular lattice T, followed by the less distorted triangular one, which is H for the aspect ratio 0.969 in the experiment. Since this aspect ratio is close to 1, the energies of H and V are very similar. The rectangular lattice, on the other hand, is the most energetic configuration and, consequently, the most unstable. Accordingly, we have never seen this type of configuration in our simulations.

We have of course to consider the pinning energy, which favors, in the absence of external force, lattice H becoming the ground state of the system, as observed in the simulations (see figure 5). However, the above calculations point out that the energy cost, due to vortex interaction, of rotating the H configuration to V is relatively small. Since the pinning energy is, by construction, comparable to the interaction energy, it is reasonable to explain the response of the system as a competition between lattices H and V.

It can also be drawn from the previous discussion that a substrate designed with a different geometry (for example, a lattice of defects with an aspect ratio closer to $2/\sqrt{3}$) could favor the

appearance of one of the lattices over the other and this might prevent the transition between them, affecting current reversal.

5. Conclusions

We have shown that current reversal in superconducting ratchets can be explained as a dynamical reconfiguration of the vortex lattice. We have presented numerical evidence of this mechanism and also shown that the interaction energy of the involved lattices is close enough to allow such reconfiguration.

The present work prompts further research in several lines. Firstly, the extension of experimental and theoretical studies on lattice transitions [26, 32, 33] to the case of moving lattices. Secondly, the analysis of the interplay between rectification and lattice configuration. We have shown that the intensity and direction of rectification can be affected not only by the shape but also by the array of defects. This could help to design rectifiers with specific responses to external forces, as well as becoming a tool to study lattice configurations. For instance, magnetoresistance, i.e. the response of the system to dc currents, is commonly used to reveal the underlying vortex lattice in superconducting films [10, 24]. Our work indicates that the response to ac currents in the presence of asymmetric artificial defects can also provide valuable information on the lattice structure.

Finally, similar ratchet mechanisms could be observed in other type of systems. The main ingredient is a lattice or complex object undergoing conformational changes as a response to external forces and in order to adapt to some anisotropic substrate. These conformation changes will depend on the sign of the force and can amplify or modify the rectification properties of the substrate. We believe that this type of generic ratchet effect could be observed in other systems with interacting particles, like colloidal suspensions or granular media.

Acknowledgments

We acknowledge funding support by Spanish Ministerio de Educación y Ciencia, grants NAN04-09087, FIS05-07392, MAT05-23924E, and MOSAICO; CAM grant S-0505/ESP/0337, and UCM-Santander. Also, computer simulations of this work were performed partly at the ‘Cluster de cálculo para Técnicas Físicas’ of UCM, funded in part by UE-FEDER program and in part by UCM and in the ‘Aula Sun Microsystems’ at UCM.

References

- [1] Reimann P 2002 *Phys. Rep.* **361** 57
- [2] Jülicher F, Ajdari A and Prost J 1997 *Rev. Mod. Phys.* **69** 1269
- [3] Serreli V, Lee C F, Kay E R and Leigh D A 2007 *Nature* **445** 523
- [4] Huang T J, Brough B, Hoa C M, Liu Y, Flood A H, Bonvallet P A, Tseng H R, Stoddarta J F, Baller M and Magonov S 2004 *Appl. Phys. Lett.* **85** 5391
- [5] Rousselet J, Solome L, Ajdari A and Prost J 1994 *Nature* **370** 446
- [6] Lee C S, Janko B, Derényi L and Barábasi A L 1999 *Nature* **400** 337
- [7] Wambaugh J F, Reichhardt C, Olson C J, Marchesoni F and Nori F 1999 *Phys. Rev. Lett.* **83** 5106
- [8] Zapata I, Bartussek R, Sols F and Hänggi P 1996 *Phys. Rev. Lett.* **77** 2292
- [9] Marconi V I 2007 *Phys. Rev. Lett.* **98** 047006

- [10] Villegas J E, Savel'ev S, Nori F, González E M, Anguita J V, García R and Vicent J L 2003 *Science* **302** 1188
- [11] Savel'ev S and Nori F 2005 *Chaos* **15** 026112
- [12] Misko V R, Savel'ev S, Rakhmanov A L and Nori F 2006 *Phys. Rev. Lett.* **96** 127004
Misko V R, Savel'ev S, Rakhmanov A L and Nori F 2007 *Phys. Rev. B* **75** 024509
- [13] Savel'ev S, Misko V, Marchesoni F and Nori F 2005 *Phys. Rev. B* **71** 214303
- [14] Van de Vondel J, de Souza Silva C C, Zhu B Y, Morelle M and Moshchalkov V V 2005 *Phys. Rev. Lett.* **94** 057003
- [15] Tinkham M 1996 *Introduction to Superconductivity* (New York: McGraw-Hill)
- [16] Savel'ev S, Marchesoni F and Nori F 2003 *Phys. Rev. Lett.* **91** 010601
Savel'ev S, Marchesoni F and Nori F 2004 *Phys. Rev. Lett.* **92** 160602
- [17] Reimann P, Kawai R, Van den Broeck C and Hänggi P 1999 *Europhys. Lett.* **45** 545
- [18] Cao F J, Dinis L and Parrondo J M R 2004 *Phys. Rev. Lett.* **93** 040603
- [19] Olson Reichhardt C J and Reichhardt C 2005 *Physica C* **432** 125
- [20] de Souza Silva C C, Van de Vondel J, Morelle M and Moshchalkov V V 2006 *Nature* **440** 651
- [21] Shalóm D E and Pastoriza H 2005 *Phys. Rev. Lett.* **94** 177001
- [22] Lu Q, Olson Reichhardt C J and Reichhardt C 2007 *Phys. Rev. B* **75** 054502
- [23] Villegas J E, González E M, González M P, Anguita J V and Vicent J L 2005 *Phys. Rev. B* **71** 024519
- [24] Martín J I, Vélez M, Nogues J and Schuller I K 1997 *Phys. Rev. Lett.* **79** 1929
- [25] Mkrtychyan G S and Shmidt V V 1972 *Sov. Phys.—JETP* **34** 195
- [26] Martín J I, Vélez M, Hoffmann A, Schuller I K and Vicent J L 1999 *Phys. Rev. Lett.* **83** 1022
- [27] Vélez M, Martín J I, Montero M I, Schuller I K and Vicent J L 2002 *Phys. Rev. B* **65** 104511
- [28] Jaccard Y, Martín J I, Cyrille M C, Velez M, Vicent J L and Schuller I K 1998 *Phys. Rev. B* **58** 8232
- [29] Zhu B Y, Van Look L, Moshchalkov V V, Marchesoni F and Nori F 2003 *Physica E* **18** 322
- [30] Martín J I, Vélez M, Hoffmann A, Schuller I K and Vicent J L 2000 *Phys. Rev. B* **62** 9110
- [31] Vélez M, Jaque D, Martín J I, Guinea F and Vicent J L 2002 *Phys. Rev. B* **65** 094509
- [32] Reichhardt C, Olson C J and Nori F 1998 *Phys. Rev. B* **57** 7937
- [33] Brown S P, Charalambous D, Jones E C, Forgan E M, Kealey P G, Erb A and Kohlbrecher J 2004 *Phys. Rev. Lett.* **92** 067004